

Article

Not peer-reviewed version

Gastric Cancer Detection with Ensemble Learning on digital pathology: Use Case of Gastric Cancer on GasHisSDB dataset

Govind Rajesh Mudavadkar , Mo Deng , [Salah Mohammed Awad Al-Heejawi](#) , [Isha Hemant Arora](#) , [Anne Breggia](#) , [Bilal Ahmad](#) , [Robert Christman](#) , Stephen T. Ryan , [Saeed Amal](#) *

Posted Date: 6 August 2024

doi: [10.20944/preprints202408.0297.v1](https://doi.org/10.20944/preprints202408.0297.v1)

Keywords: Cancer Detection; Machine Learning; Gastrointestinal Cancer; Deep Learning; Histopathology



Preprints.org is a free multidiscipline platform providing preprint service that is dedicated to making early versions of research outputs permanently available and citable. Preprints posted at Preprints.org appear in Web of Science, Crossref, Google Scholar, Scilit, Europe PMC.

Copyright: This is an open access article distributed under the Creative Commons Attribution License which permits unrestricted use, distribution, and reproduction in any medium, provided the original work is properly cited.

Disclaimer/Publisher's Note: The statements, opinions, and data contained in all publications are solely those of the individual author(s) and contributor(s) and not of MDPI and/or the editor(s). MDPI and/or the editor(s) disclaim responsibility for any injury to people or property resulting from any ideas, methods, instructions, or products referred to in the content.

Article

Gastric Cancer Detection with Ensemble Learning on digital pathology: Use Case of Gastric Cancer on GasHisSDB dataset

Govind Rajesh Mudavadkar ¹, Mo Deng ², Salah Mohammed Awad Al-Heejawi ³, Isha Hemant Arora ⁴, Anne Breggia ⁵, Bilal Ahmad ⁶, Robert Christman ⁷, Ryan T Stephen ⁸ and Saeed Amal ^{9,*}

¹ Khoury College of Computer Sciences, Northeastern University, Boston, MA 02115, USA; mudavadkar.g@northeastern.edu

² College of Engineering, Northeastern University, Boston, MA 02115, USA; m.deng@northeastern.edu

³ College of Engineering, Northeastern University, Boston, MA 02115, USA; s.al-heejawi@northeastern.edu

⁴ Khoury College of Computer Sciences, Northeastern University, Boston, MA 02115, USA; arora.isha@northeastern.edu

⁵ MaineHealth Institute for Research, Scarborough, ME 04074, USA; anne.breggia@mainehealth.org

⁶ Maine Medical Center, Portland, ME 04102, USA; bilal.ahmad@spectrumhcp.com

⁷ Maine Medical Center, Portland, ME 04102, USA; robert.christman@spectrumhcp.com

⁸ Maine Medical Center, Portland, ME 04102, USA; stephen.ryan@mainehealth.org

⁹ The Roux Institute, Department of Bioengineering, College of Engineering at Northeastern University, Boston, MA 02115, USA; s.amal@northeastern.edu

* Correspondence: Saeed Amal; s.amal@northeastern.edu

Simple Summary: Gastric cancer is a major worldwide health concern, underscoring the importance of early detection to enhance patient outcomes. Traditional histological analysis, while considered the gold standard, is labor-intensive and manual. Deep learning (DL) is a potential approach, but existing models fail to extract all visual data required for successful categorization. This work overcomes these constraints by using ensemble models that mix different deep learning architectures to improve classification performance for stomach cancer diagnosis. Using the Gastric Histopathology Sub-size Images Database, the ensemble models obtained an average accuracy of more than 99% at various resolutions. ResNet50, VGGNet, and ResNet34 beat EfficientNet and VitNet, with the ensemble model continuously delivering higher accuracy. These findings show that ensemble models may accurately detect important characteristics from smaller picture patches, allowing pathologists to diagnose stomach cancer early and increasing patient survival rates.

Abstract: Gastric cancer has become a serious worldwide health concern, emphasizing the crucial importance of early diagnosis measures to improve patient outcomes. While traditional histological image analysis is regarded as the clinical gold standard, it is labor-intensive and manual. Recognizing this problem, there has been a rise in interest in using computer-aided diagnostics tools to help pathologists with their diagnostic efforts. In particular, deep learning (DL) has emerged as a promising solution in this sector. However, current DL models are still restricted in their ability to extract extensive visual characteristics for correct categorization. To tackle this limitation, this study proposes the use of ensemble models, which incorporate the capabilities of several deep learning architectures and use aggregate knowledge of many models to improve classification performance, allowing for more accurate and efficient gastric cancer detection. To see how well these proposed models performed, this study compared them to other works, all of which were based on the Gastric Histopathology Sub-size Images Database, a publicly available dataset for gastric cancer. This research demonstrated that the ensemble models achieved high detection accuracy across all sub-databases, with an average accuracy exceeding 99%. Specifically, ResNet50, VGGNet, and ResNet34 performed better than EfficientNet and VitNet. For the 80×80 pixel sub-database, ResNet34 exhibited an accuracy of approximately 93%, VGGNet achieved 94%, and the ensemble model excelled with 99%. In the 120×120 pixel sub-database, the ensemble model showed 99% accuracy, VGGNet 97%, and ResNet50 approximately 97%. For the 160×160 pixel sub-database, the ensemble model again achieved 99% accuracy, VGGNet 98%, ResNet50 98%, and EfficientNet 92%, highlighting the ensemble model's superior performance across all resolutions. Overall, the

ensemble model consistently provided an accuracy of 99% across the three sub-pixel categories. These findings showed that ensemble models may successfully detect critical characteristics from smaller patches and achieve high performance. The findings will help pathologists diagnose gastric cancer using histopathological images, leading to earlier identification and higher patient survival rates.

Keywords: cancer detection; machine learning; gastrointestinal cancer; deep learning; histopathology

1. Introduction

The GI tract, spanning 25 feet from the oral cavity to the anus, transports ingested substances. The digestive process begins with the oesophagus and continues through the stomach and small intestines, extracting important nutrients. Waste is then eliminated through the colon and rectum. [1,2] Tumors in these organs often result from aberrant cell growth caused by DNA changes.[4] Mutations can be caused by a variety of reasons, including health conditions, genetics, lifestyle. The uncontrolled proliferation of malignant cells in the gastrointestinal system is caused by genetic, environmental, and lifestyle factors that interact. Common gastrointestinal (GI) cancers include Esophageal Cancer, Colorectal Cancer, Gastric Cancer, Bile Duct Cancer, Anal Cancer, Colon Cancer, Gallbladder Cancer, Pancreatic Cancer, Gastrointestinal Stromal Tumours, Liver Cancer, Rectal Cancer, Gastric Cancer, and Small Intestine Cancer. In 2020, gastric cancer was one of the top three most common cancers in 19 nations, with around 1.1 million cases reported (720,000 men, 370,000 females). Early identification of GI cancer aids in cancer treatment and reduces health-related complications.

Traditional approaches for identifying cancer include estimating body fat percentage and thereafter correlating it to cancer. Other methods include identifying common microbes associated with cancer in food. Another way is the use of Indocyanine Green (ICG) in gastrointestinal surgery, which is gaining popularity, particularly for lymph node diagnosis and operative field imaging [13,14].

However, pathologists must physically assess tissue samples, which is a tough, time-consuming, and subjective procedure. Moreover, different pathologists may provide different results, making the analysis susceptible to errors. The accuracy of histopathological analysis is heavily dependent on the pathologists' experience and knowledge, making the manual process susceptible to mistakes such as incorrect detection and diagnosis. Furthermore, a scarcity of pathologists creates significant delays in examining patient cases, potentially leading to late cancer discovery [15,16].

Various computer-aided detection (CAD) strategies have been investigated for the diagnosis of gastric cancer utilizing histopathological imaging. For more than 30 years, researchers have studied computer-aided diagnosis in gastroenterology, creating datasets from endoscopic images using various methodologies. The most widely researched issue is the identification of aberrant pathological signs in a specific location of the GI tract, notably polyps. There has also been research on detecting and categorizing disorders throughout the GI system, such as clinical findings, anatomical markers, and therapeutic therapies [3].

2. Materials and Methods

2.1. Literature Reviews

Various computer-aided detection (CAD) strategies have been investigated for the diagnosis of gastric cancer utilizing histopathological imaging. For more than 30 years, researchers have studied computer-aided diagnosis in gastroenterology, creating datasets from endoscopic images using various methodologies. The most widely researched issue is the identification of aberrant pathological signs in a specific location of the GI tract, notably polyps. There has also been research on detecting and categorizing disorders throughout the GI system, such as clinical findings, anatomical markers, and therapeutic therapies [3]. During the first 20 years of development, image

processing required extracting features using various approaches and then categorizing them using statistical methods [19]. These characteristics were divided into three categories: spatial, frequency, and high-level descriptors. Spatial characteristics were retrieved using pixel-based and histogram techniques, whilst frequency information was collected using Fourier and wavelet transform algorithms. High-level characteristics were retrieved with edge and region-based methods. Statistical machine-learning approaches were frequently employed to categorize these characteristics.

Later, machine learning (ML) is commonly used in CAD to diagnose gastric cancer by extracting handmade elements such as color, texture, and form. For this purpose, support vector machines (SVM), random forests, and Adaboost are among the most frequently employed machine learning classifiers. In recent research, deep learning has been utilized to automate the feature selection process. Several studies have shown that deep convolutional neural networks (CNN) excel at tasks such as recognizing and segmenting histopathological images related to cancer, metastasis, and genetic mutation analysis. Some investigations have indicated that these networks perform similarly to human pathologists [7,8].

Deep learning techniques have advanced significantly over the past decade, notably with the CNN architecture. This design allows for the extraction and categorization of spatial as well as high-level features, making it a major area of study for academia. Several solutions have been proposed, including hybrid approaches based on CNN attributes, transfer learning, the development of novel CNN models, and research into other deep learning networks [20].

Gastroenterology CAD research has a long history and covers a wide range of topics. For studies involving the classification of the KvasirV2 and HayperKvasir datasets, which were employed in the studies conducted [19,20], Melaku et al. (2019) utilized VGGNet and InceptionV3 to classify the Hyper KVASIR dataset with 98% accuracy using SVM. M Hmoud et al. (2020) evaluated GoogLeNet, ResNet-50, and AlexNet on the KVASIR dataset, with AlexNet outperforming the others and achieving 97% accuracy. Yogapriya et al. (2021) used VGG16, ResNet-18, and GoogLeNet on the KVASIR v2 dataset, with VGG16 leading the way with an accuracy of about 96.33%. Furthermore, Zenebe et al. (2022) proposed a unique deep convolutional neural network (CNN) with a spatial attention mechanism for categorizing gastrointestinal (GI) illnesses. [17,18]. When evaluated on a dataset of 12,147 GI images, the model scored an astounding 92.84% accuracy. This study emphasizes the importance of using pre-trained models in the correct diagnosis of gastrointestinal disorders, showcasing numerous methodologies and achieving significant advances in this sector.

To assess how well the proposed models worked, this research evaluated them using the recently available Gastric Histopathology Sub-size Image Database (GasHisSDB) [6]. The main contributions of this study are: 1. The development of effective deep ensemble learning models for detecting gastric cancer that outperform current research on the GasHisSDB dataset. 2. Deep ensemble learning's ability to successfully identify gastric histology images with lower resolution, perhaps resulting in fewer digital scanners, data storage, and computer servers needed for histopathology activities. This may increase the chance of early detection of gastric cancer and enhance rates of patient survival [9,10].

2.2. Dataset Description



Figure 1. Process of extraction of the Histopathology Image.

The stomach Histopathology Sub-size Image Database (GasHisSDB) comprises 600 pictures of stomach cancer pathology obtained from a patient's pathological slides from a specific section of the Gastrointestinal tract, each measuring 2048x2048 pixels. The images were obtained by scanning with a NewUsbCamera at a magnification of 20. Four pathologist from Longhua Hospital at the Shanghai University of Traditional Chinese Medicine then provided tissue-specific labeling. In conjunction with five Northeastern University biomedical experts, the photos were cropped into 245,196 sub-sized gastric cancer pathology images. Two qualified pathologist from Liaoning Cancer Hospital and Institute calibrated these pictures. The dataset was then classed as aberrant or normal, with photographs reduced to three different sizes (160x160, 120x120, and 80x80) for each group. The dataset of gastrointestinal images is separated into three sizes: 80x80, 120x120, and 160x160. Each size category is further classified into two groups: Abnormal and Normal. The 80x80 size category has 81,390 photos, with 34,350 classed as Abnormal and 47,040 labeled as Normal. Moving on to the 120x120 size category, there are 65,260 photos altogether, with 24,800 rated as Abnormal and 40,460 as Normal. Finally, in the 160x160 size group, there are 33,272 photos, with 13,117 classified as Abnormal and 20,155 as Normal.

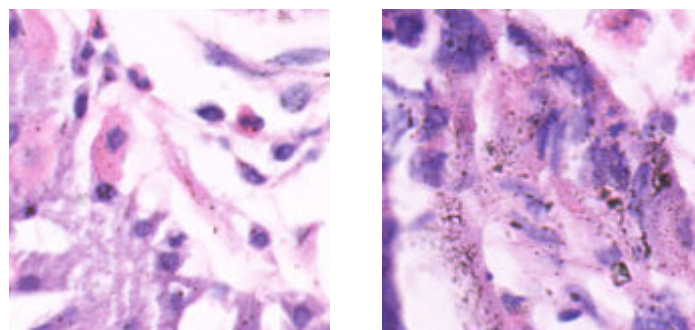


Figure 2. Examples of histopathological Gastric images. (a) Normal tissue and (b) Abnormal tissue.

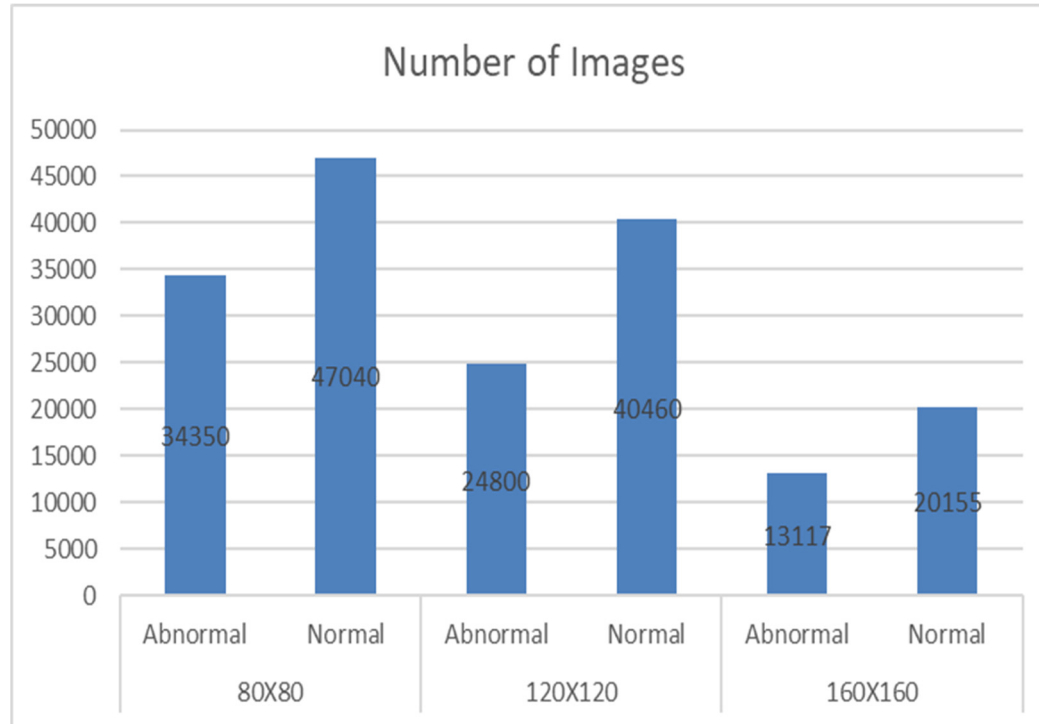


Table 1. Summarises the total number of images for every subclass in an experiment setup.

2.3. Methodology Overview

In this work, CNN architectures utilizing transfer learning and ensemble approaches were demonstrated to detect gastric cancer patches. The process is divided into four major steps: (1) creating the dataset through eliminating empty patches and augmenting, (2) tailoring pre-trained networks or base models, (3) choosing the most effective base models to form ensemble models, and (4) assessing and presenting the models using different metrics and the class activation map.

To enhance the model performance, data preprocessing was conducted to create a more balanced dataset by removing non-informative empty patches as the presence of these empty patches would bias the training process and therefore jeopardize the model performance. After empty patches removal, data augmentation was employed to increase the dataset size for training.

2.4. Empty Patch Removal Process

Empty patches are defined as those where more than half of the pixels have an RGB intensity value greater than 230 across all channels. The following is an overview of the empty patch removal procedure, including the proportion of empty patches deleted. In the 120x120 resolution dataset, 15.92% of patches were removed from the abnormal subclass, while 45.01% were removed from the normal subclass. For the 160x160 resolution dataset, 14.77% of patches were removed from the abnormal subclass, and 44.23% were removed from the normal subclass. In the 80x80 resolution dataset, 17.45% of patches were removed from the abnormal subclass, and 45.54% were removed from the normal subclass. After removing these empty patches, the remaining patches were subjected to data training of the model

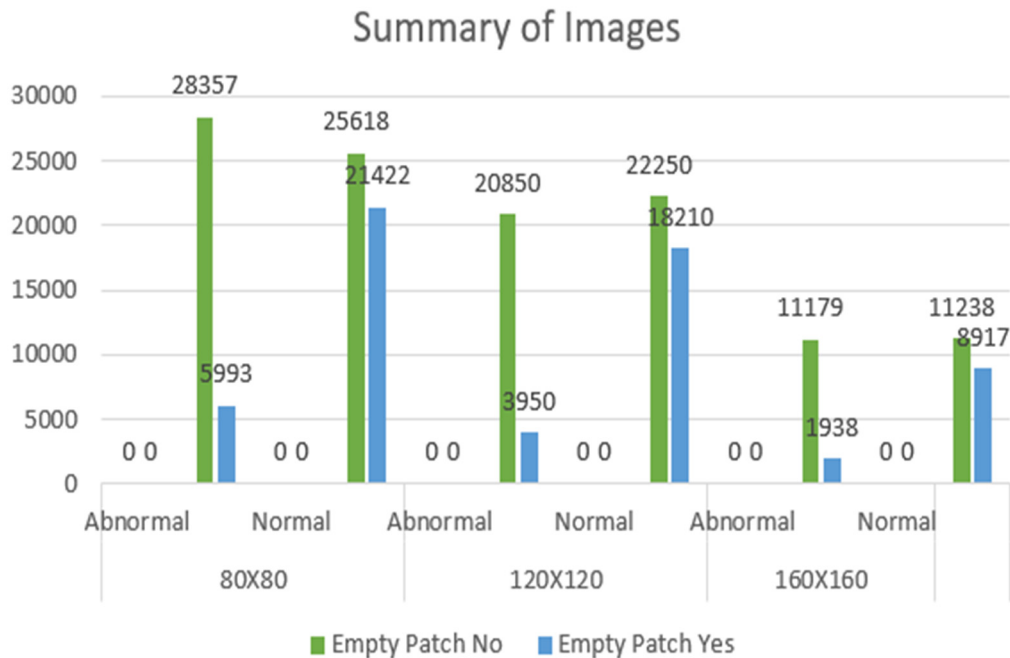


Table 2. Summarises the total number of the Empty and Non-Empty Patch Images in the Dataset.

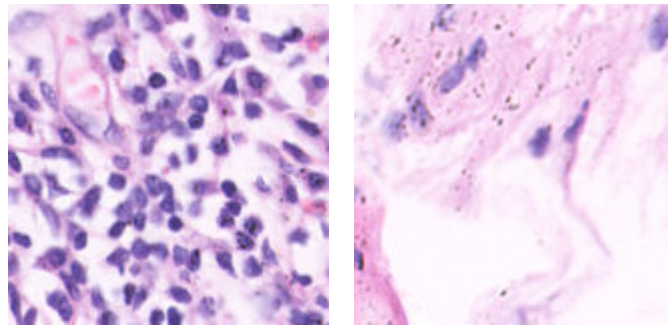


Figure 3. The pictures above exhibit examples of histopathology: non-empty and empty patch images on the left and right, respectively.

2.5. Pretrained networks as Base Models

Convolutional Neural Networks (CNNs) have played an important role in numerous applications since deep learning's inception, due to continual advances in strength, efficiency, and adaptability. CNNs are an excellent illustration of this breakthrough, as they are particularly built for computer vision problems and use convolutional layers inspired by natural visual processes. Multiple CNN structures have evolved throughout time, each improving accuracy, speed, and overall performance, and are usually compared to the ImageNet project, a massive visual database that promotes advancements in computer vision.

Historically, training CNNs from scratch required significant computer resources and time. Transfer learning (TL) provides a practical shortcut by exploiting prior information from trained models to accelerate optimization and perhaps improve classification accuracy. TL entails transferring weights from pre-trained models, using insights acquired from varied datasets, and speeding training processes to improve model accuracy, particularly in complicated architectures [11,12].

ResNet34 Architecture:

ResNet34 is a member of the Residual Networks (ResNet) family, which was introduced by He et al. in 2015. ResNet34 uses residual learning to address the issue of vanishing gradients, which is common in deep neural networks. This design is made up of 34 layers, with shortcut connections that allow gradients to flow straight across the network. These residual connections enable the training of very deep networks by overcoming the degradation issue. ResNet34 strikes a balance between depth and computational efficiency, beating shallower networks while maintaining manageable computational costs.

ResNet34 is a variation of ResNet, a CNN architecture created by Microsoft Research. ResNet34 includes 34 layers and uses residual connections to overcome the vanishing gradient problem, making training more efficient. ResNet models are popular due to their efficacy in a variety of applications.

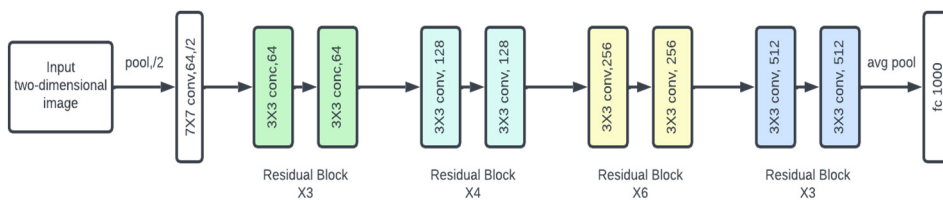


Figure 4. ResNet34 Model Architecture.

ResNet50 Architecture:

ResNet50 is a 50-layer version of the ResNet architecture, deeper than ResNet34. This enhanced depth can improve performance on certain tasks, but it also necessitates more computational resources for training.

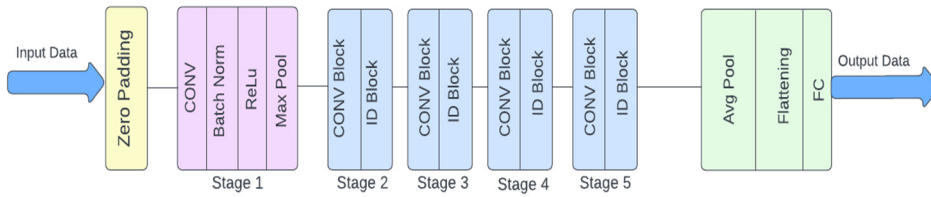


Figure 5. ResNet50 Model Architecture.

VGGNet16 Architecture:

The Visual Geometry Group (VGG) at the University of Oxford developed VGGNet16, a deep CNN architecture. It is well-known for being both simple and successful in picture classification applications. VGGNet16 is made up of 16 layers, the first 13 of which are convolutional, followed by three fully connected layers. Each convolutional layer has a 3x3 kernel, and max-pooling layers are used after a sequence of convolutional layers to minimize spatial dimensions. Although VGGNet16 has a huge number of parameters, which makes it computationally costly, it achieves good accuracy on benchmark datasets thanks to its deep architecture and consistent layer design.

VGGNet, created by the Visual Geometry Group at the University of Oxford, is renowned for its simplicity. It is mostly composed of layered convolutional layers with 3x3 kernels and max-pooling layers. VGGNet includes several variations, including VGG16 and VGG19, which differ in the number of layers.



Figure 6. VGGNet16 Model Architecture.

Efficientnet Architecture:

EfficientNet is a class of CNN models developed by Google AI that outperforms earlier models using fewer parameters and FLOPs. They employ a novel scaling technique to improve network depth, breadth, and resolution for improved resource management.

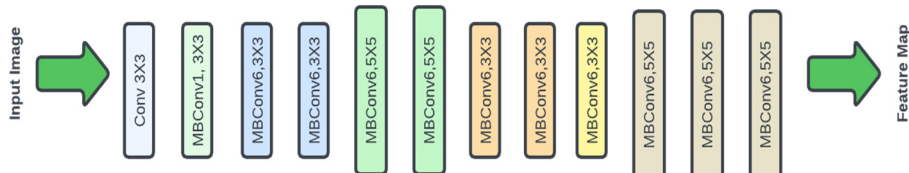


Figure 7. EfficientNet Model Architecture.

VitNet Architecture:

The Vision Transformer is a novel CNN architecture created by Google Research that employs self-attention techniques seen in transformer topologies. Rather than employing convolutional layers like typical CNNs, ViT employs a transformer encoder, which allows it to recognize relationships across large distances in pictures. This method has shown outstanding results in several computer vision tasks, particularly when trained on large datasets.

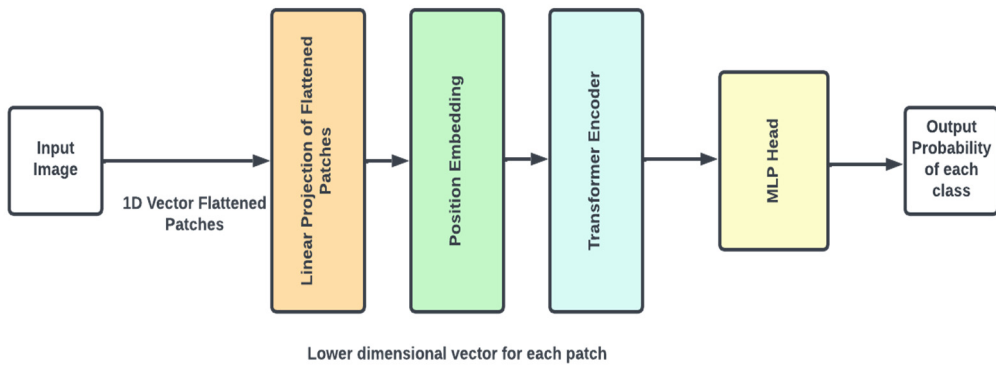


Figure 8. VITNet Model Architecture.

Ensemble Architecture:

Convolutional neural networks (CNNs) and transfer learning have significantly increased neural network performance, but there is still potential for improvement. This article proposes the use of ensemble methods to improve the effectiveness of the three models that have been pre-trained. Ensemble learning, a machine learning and statistics-based approach combines the skills of many algorithms to extract relevant insights from data[10].

During this analysis, stacking was determined to be the most appropriate method. This requires training various ML algorithms on the info before merging them to create a composite algorithm capable of successfully combining their input.

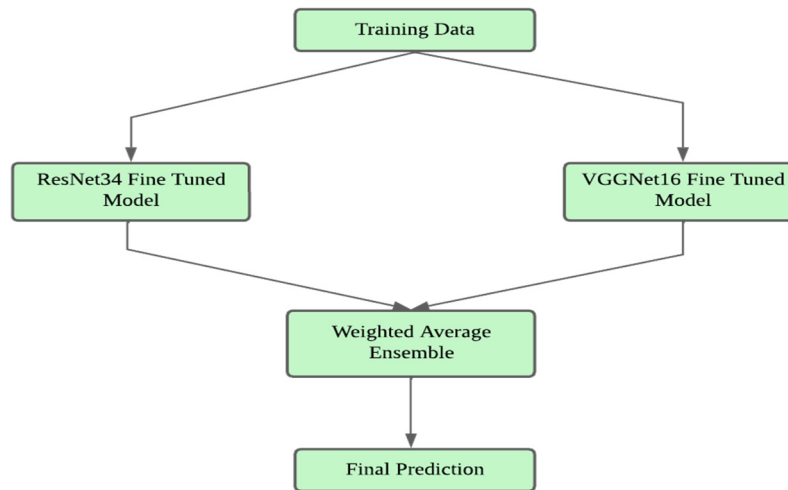


Figure 9. Ensemble Model Architecture.

In this research, ensemble model architecture was used using ResNet34 and VGGNet16 as basis models. Initially, each model was trained independently to determine its unique performance. Then

selected the best-performing epochs for each model based on validation accuracy. The best-performing epochs were then used to build the ensemble model.

To improve the robustness and generalizability of the ensemble techniques, cross-validation is used. During each fold of the cross-validation approach, the research utilized the best weights from the previous folds to train the ensemble. For example, if cross-validation was done on fold 1, the best epochs from folds 2, 3, 4, and 5 of ResNet34 and VGGNet16 were used to establish the ensemble model.

The ensemble model architecture was created to leverage on the complementary characteristics of ResNet34 and VGGNet16. ResNet34, with its residual connections, successfully mitigates the vanishing gradient problem, allowing for deeper network training. In contrast, VGGNet16, noted for its simplicity and constant layer architecture, excels in capturing fine-grained characteristics. By integrating both models, the ensemble takes use of VGGNet16's comprehensive feature extraction and ResNet34's depth-wise learning capabilities.

Training the ensemble model entailed freezing the early layers of both base models to preserve their pre-trained feature extraction capabilities while fine-tuning the subsequent layers to fit to the unique dataset. This hybrid strategy enabled the ensemble model to outperform individual models, as indicated by improved accuracy and resilience across many validation criteria. In summary, the proposed ensemble model, which included ResNet34 and VGGNet16, showed considerable performance increases. The strategic use of cross-validation and the incorporation of complementary model architectures demonstrate the effectiveness of ensemble techniques in deep learning applications.

2.6. Experimental Setting

The data was divided into training and validation sets. Each network was trained for 20 epochs using 5-fold cross-validation to create the model. The weights from the epoch with the best validation accuracy were chosen as the final representations for each model. Various metrics were then employed to assess accuracy, followed by many objective assessment factors to determine overall performance.

3. Results

The performance evaluation criteria used include accuracy, sensitivity, specificity, Jaccard index, and area under the curve (AUC). Positive samples are those that include abnormal or malignant patches, whereas negative samples contain normal or healthy patches. The phrases true positive (TP), false positive (FP), true negative (TN), and false negative (FN) are used to describe the various prediction results.

1. Accuracy: Accuracy is the ratio of properly identified samples to the total number of samples. It's computed as:

$$\text{Accuracy} = \frac{(TP+TN)}{(TP+TN+FP+FN)} \quad (1)$$

2. Sensitivity (Recall): Sensitivity, also known as recall, is the proportion of real positive samples that the model properly identifies. It's provided by:

$$\text{Sensitivity} = \frac{(TP)}{(TP+FN)} \quad (2)$$

3. Specificity refers to the fraction of real negative samples properly detected by the model. It's computed as:

$$\text{Specificity} = \frac{(TN)}{(TN+FP)} \quad (3)$$

4. The Jaccard index, commonly known as the Intersection over Union (IoU), assesses the similarity between expected and observed positive samples. It's provided by:

$$\text{Jaccard index,} = \frac{(TP)}{(TP+FP+FN)} \quad (4)$$

5. Area Under the Curve (AUC): The area under the receiver operating characteristic (ROC) curve, or AUC, relates the true positive rate (sensitivity) to the false positive rate (1 - specificity). A higher AUC implies improved model performance.

By examining these measures, a thorough picture of the model's performance can be acquired, particularly in discriminating between aberrant (positive) and normal (negative) data.

When analyzing the success of machine learning models, performance measures must be considered. These metrics provide numerical numbers that indicate the overall performance of a statistical or machine-learning technique. In classification tasks, performance measures evaluate the model's capacity to accurately categorize data points as well as its consistency in producing the right classifications. Classification accuracy and F1-score are both measures of classification task accuracy, whereas AUC reflects the model's overall ability to forecast accurately. The study's findings, which were obtained by examining these performance metrics, are shown in the table below.

Table 3. The effectiveness of the several deep learning models was assessed using an 80-pixel sub-database, displayed above. The most stunning results are shown in bold.

Model	Fold	Train Accuracy	Train Loss	Val Accuracy	Val Loss	Jaccard Index	AUC	Specificity	Sensitivity
Resnet34	1	98.7508	0.0331	93.6131	0.2175	0.7447	0.9719	0.9604	0.8494
	2	97.8192	0.0604	93.7206	0.2092	0.7472	0.9717	0.9638	0.8427
	3	98.8546	0.0329	93.8111	0.2210	0.7384	0.9760	0.9699	0.8204
	4	97.7773	0.0596	93.8226	0.1724	0.7466	0.9777	0.9625	0.8491
	5	98.1767	0.0487	93.7910	0.2399	0.7640	0.9754	0.9518	0.8900
ResNet50	1	98.4818	0.0409	93.7408	0.1936	0.8763	0.8979	0.9682	0.8277
	2	96.2419	0.0958	94.2439	0.1880	0.8860	0.9069	0.9703	0.8435
	3	98.4410	0.0413	93.4971	0.2024	0.8742	0.9042	0.9577	0.8508
	4	97.0654	0.0769	92.7688	0.2016	0.8601	0.9071	0.9431	0.8711
	5	93.5411	0.1673	93.8459	0.1869	0.8772	0.9064	0.9648	0.8480
VitNet	1	83.6243	0.3631	83.7591	0.3555	0.6945	0.7132	0.9347	0.4916
	2	82.9835	0.3816	84.2836	0.3490	0.6969	0.7076	0.9493	0.4660
	3	78.4974	0.4755	78.8656	0.4560	0.5946	0.5054	0.9988	0.0121
	4	82.5612	0.3898	84.2841	0.3505	0.6986	0.7015	0.9488	0.4542
	5	78.3217	0.5231	77.4105	0.5353	0.5674	0.5	1	0
VggNet	1	98.7371	0.0366	93.7591	0.2579	0.8763	0.9746	0.9747	0.8053
	2	96.2693	0.0969	94.3341	0.1785	0.8868	0.9757	0.9738	0.8353
	3	98.5683	0.0417	93.9220	0.2120	0.8763	0.9751	0.9720	0.8178
	4	94.3224	0.1519	93.7681	0.1621	0.8756	0.9733	0.9685	0.8245
	5	98.3636	0.0487	93.7910	0.2329	0.8768	0.9724	0.9693	0.8302
EfficientNet	1	74.9474	0.5035	75.4057	0.5142	0.6094	0.7478	0.7172	0.7784
	2	82.4435	0.3866	83.0474	0.3685	0.6829	0.6726	0.9421	0.4030
	3	81.0359	0.4139	82.3709	0.3855	0.6704	0.6346	0.9463	0.3229
	4	82.3379	0.3879	84.2231	0.3531	0.6975	0.6725	0.9419	0.4030
	5	82.6571	0.3805	83.5210	0.3651	0.6944	0.6816	0.9401	0.4232
Ensemble	1	98.3587	0.0436	99.3430	0.0252	0.9867	0.9904	0.9957	0.9850
	2	98.5187	0.0410	99.2421	0.0211	0.9839	0.9875	0.9962	0.9787
	3	98.6001	0.0384	99.2056	0.0237	0.9836	0.9898	0.9936	0.9861
	4	97.9234	0.0627	97.8197	0.0651	0.9562	0.9642	0.9886	0.9398
	5	98.5642	0.0390	99.0869	0.0221	0.9823	0.9866	0.9943	0.9789

Table 4. The effectiveness of the several deep learning models was assessed using a 120-pixel sub-database, displayed above. The most stunning results are shown in bold.

Model	Fold	Train Accuracy	Train Loss	Val Accuracy	Val Loss	Jaccard Index	AUC	Specificity Sensitivity
Resnet34	1	98.8627	0.0327	96.8167	0.1097	0.8347	0.9879	0.9812 0.9075
	2	99.2847	0.0187	97.0297	0.1327	0.8444	0.9815	0.9884 0.8884
	3	98.9145	0.0336	96.9364	0.1025	0.8392	0.9907	0.9901 0.8762
	4	99.1640	0.0234	96.4475	0.1208	0.8175	0.9879	0.9836 0.8778
	5	99.2957	0.0214	96.6893	0.1074	0.8149	0.9897	0.9877 0.8642
ResNet50	1	99.5552	0.0125	96.7257	0.1120	0.9316	0.9518	0.9756 0.9281
	2	99.2449	0.0213	96.9856	0.1156	0.9372	0.9254	0.9951 0.8557
	3	99.7229	0.0089	97.0930	0.1198	0.9388	0.9493	0.9833 0.9154
	4	99.5007	0.0142	96.8166	0.1253	0.9339	0.9379	0.9853 0.8905
	5	99.5042	0.0147	97.0748	0.0995	0.9379	0.9406	0.9860 0.8951
VitNet	1	86.6963	0.3109	87.4715	0.2875	0.7518	0.7395	0.9488 0.5301
	2	84.6948	0.3495	86.1826	0.3185	0.7254	0.7123	0.9470 0.4775
	3	82.2817	0.4486	81.7531	0.4287	0.6310	0.5	1 0
	4	85.7447	0.3298	87.9123	0.2929	0.7581	0.7607	0.9464 0.5750
	5	84.2084	0.3465	86.3265	0.3085	0.7231	0.6767	0.9582 0.3951
VggNet	1	76.6185	0.4764	75.6162	0.5053	0.6152	0.7657	0.7776 0.7538
	2	88.3740	0.2758	89.1768	0.2611	0.7889	0.7476	0.9592 0.5361
	3	88.1351	0.2822	88.3388	0.2732	0.7756	0.7372	0.9605 0.5139
	4	86.6576	0.3140	88.2826	0.2813	0.7673	0.6979	0.9591 0.4368
	5	88.3702	0.2745	88.4198	0.2781	0.7779	0.7460	0.9594 0.5325
EfficientNet	1	99.1949	0.0265	96.8167	0.1372	0.9340	0.9878	0.9867 0.8818
	2	99.8978	0.0054	96.9416	0.1716	0.9363	0.9886	0.9873 0.8884
	3	98.4339	0.0464	97.1824	0.1130	0.9403	0.9883	0.9901 0.8897
	4	96.4544	0.1011	96.0322	0.1098	0.9176	0.9860	0.9757 0.8905
	5	99.8366	0.0061	96.9614	0.1410	0.9338	0.9902	0.98363 0.9005
Ensemble	1	97.2581	0.0728	97.6125	0.0646	0.9501	0.9593	0.9853 0.9332
	2	97.7973	0.0622	98.1738	0.0533	0.9627	0.9647	0.9913 0.9381
	3	97.7894	0.0603	97.8756	0.0618	0.9531	0.9636	0.9874 0.9399
	4	97.8457	0.0625	97.5778	0.0685	0.9486	0.9549	0.9876 0.9223
	5	98.9735	0.0316	99.4250	0.0226	0.9872	0.9895	0.9965 0.9826

Table 5. The effectiveness of the several deep learning models was assessed using a 160-pixel sub-database, displayed above. The most stunning results are shown in bold.

Model	Fold	Train Accuracy	Train Loss	Val Accuracy	Val Loss	Jaccard Index	AUC	Specificity Sensitivity
Resnet34	1	99.6311	0.0132	97.9807	0.0648	0.8949	0.9961	0.9887 0.9398
	2	99.5496	0.0148	98.1776	0.0656	0.9022	0.9913	0.9922 0.9341
	3	99.7337	0.0083	98.1038	0.0535	0.8928	0.9976	0.9912 0.9308
	4	97.1184	0.0896	97.2005	0.0821	0.8665	0.9931	0.9806 0.9361
	5	99.5437	0.0213	98.4187	0.0738	0.9105	0.9929	0.9862 0.9739
ResNet50	1	99.3660	0.0288	98.4396	0.0579	0.9678	0.9739	0.9904 0.9573
	2	99.5842	0.0170	98.3143	0.0592	0.9628	0.9719	0.9894 0.9544
	3	99.8263	0.0066	98.1038	0.0776	0.9599	0.9684	0.9874 0.9494
	4	99.9538	0.0018	97.9348	0.0743	0.9574	0.9620	0.9903 0.9338
	5	99.7718	0.0112	98.3708	0.0625	0.9648	0.9832	0.9839 0.9826
VitNet	1	82.2614	0.4526	81.6888	0.4532	0.6295	0.5	1 0
	2	84.4919	0.3426	86.2870	0.3141	0.7307	0.6980	0.9555 0.4405

	3	81.9212	0.4638	83.0248	0.4527	0.6543	0.5	1	0
	4	84.3706	0.3502	84.6718	0.3393	0.6977	0.6841	0.9498	0.4184
	5	82.0483	0.3951	86.3919	0.3069	0.7274	0.6337	0.9776	0.2898
VggNet	1	77.3246	0.4784	76.5826	0.4820	0.6291	0.7732	0.7643	0.7822
	2	90.0875	0.2296	93.0702	0.1838	0.8607	0.7924	0.9604	0.6244
	3	91.0623	0.2155	92.8018	0.1911	0.8572	0.8139	0.9641	0.6636
	4	91.0069	0.2178	93.0925	0.1655	0.8589	0.8168	0.9628	0.6709
	5	91.4476	0.2077	92.0146	0.1945	0.8444	0.8186	0.9659	0.6712
EfficientNet	1	99.9769	0.0014	98.2101	0.1121	0.9623	0.9946	0.9915	0.9398
	2	99.6882	0.0098	97.9498	0.0795	0.9584	0.9944	0.9952	0.9088
	3	98.8773	0.0347	97.9683	0.0896	0.9579	0.9921	0.9934	0.9122
	4	99.2738	0.0244	97.2005	0.0940	0.9464	0.9912	0.9834	0.9243
	5	99.6692	0.0091	98.1312	0.0814	0.9586	0.9948	0.9896	0.9391
Ensemble	1	98.4785	0.0412	98.8067	0.0313	0.9751	0.9829	0.9910	0.9749
	2	99.0877	0.0268	98.9066	0.0325	0.9753	0.9775	0.9955	0.9594
	3	99.1203	0.0298	99.1873	0.0260	0.9830	0.9866	0.9945	0.9787
	4	99.4813	0.0150	99.7246	0.0079	0.9942	0.9964	0.9977	0.9952
	5	98.9165	0.0319	99.3291	0.0245	0.9836	0.9901	0.9948	0.9855

4. Discussion

In this work, the proposed model was trained on datasets with varied picture sizes, such as 80x80 and 120x120 and 160X160. Findings highlights the critical significance of ongoing innovation and exploration in increasing medical machine learning and hence improving healthcare practices. Notably, the findings shows that the top five ensemble models had high detection accuracy across all sub-databases. The overall ensemble model demonstrated the highest accuracy, surpassing the performance of VGGNet, ResNet34, and ResNet50, which also outperformed VitNet and EfficientNet. The only exception was in the 160 × 160 sub-database, where EfficientNet achieved an accuracy of 92%. By combining multidisciplinary techniques and technology breakthroughs, can pave the way towards a future in which early and precise identification of gastrointestinal disorders is not only achievable but also common practice in protecting human health and well-being.

This deliberate method was used to assist the model build a solid knowledge of multiple picture dimensions, making it more flexible to a variety of real-world scenarios. Nonetheless, it is worth noting that proposed model's knowledge may have been expanded much more with greater computing resources. Greater computational capability might have enabled a more in-depth examination of the dataset's intricacies, as well as the discovery of insights beyond existing capabilities.

These advanced methodologies offer various structures and improvement tactics that may increase the efficacy of the model. Time restrictions precluded the incorporation of these algorithms into the current system; nonetheless, their use holds great promise for improving cancer detection techniques.

This research prioritizes in innovation and placing people at the heart of the research. The objective is to make research applications as user-friendly as possible while also emphasizing how they might benefit medical practitioners. This research strive to integrate the most recent research work with practical applications, avoiding plagiarism and crafting a research story that is honest and true to research's commitment to expanding scientific understanding.

4.1. Future Directions

In the future, focus will be on two major goals: developing an easy-to-use web app for cancer detection and expanding current algorithms to include new forms of cancer. The primary goal of this research is to develop a model that will work for all forms of cancer, not just specific ones. This will be accomplished by utilizing many data sources and innovative algorithms to obtain a thorough

understanding of cancer, hence assisting healthcare professionals with diagnosis. By integrating multidisciplinary methodologies and capitalizing on technological developments, probably will work towards that in future in which early and precise identification of GI problems is not only possible, but also the standard for protecting human health and well-being.

5. Conclusion

Detecting and diagnosing gastrointestinal (GI) illnesses is critical for human health, yet it can be challenging owing to limited medical competence and expensive expenses. Using machine learning, particularly deep learning techniques, has the potential to increase the speed and accuracy of GI illness identification. This research study investigated the efficiency of ensemble approaches using five pre-trained models on the Gastric Histopathology Sub-size Image Database (GasHisSDB), which comprises a diverse set of pictures in various pixel sizes and categories. Considerable boost in prediction accuracy can be seen when utilizing ensemble learning, which combines the predictive skills of several models, as opposed to using individual models and previous studies that used comparable datasets. This demonstrates the potential of ensemble approaches to improve the capabilities of medical machine learning systems, resulting in more effective and precise diagnoses.

Current approach is based on transfer learning, a technique that improves model learning by leveraging knowledge from previously trained models. Moreover employed an ensemble strategy to improve performance by merging various classifiers. Following a rigorous review, current approach revealed a great accuracy on the test dataset, exceeding current evaluation techniques. This demonstrates how deep learning may help alleviate the pressure on healthcare systems while also improving human health outcomes. [21,22]

In this study, advanced deep ensemble learning models were created that used transfer learning from multiple pre-trained networks, including VitNet, EfficientNet, VGGNet, ResNet34, and ResNet50, to improve stomach cancer diagnosis. The study found that using base models in ensemble learning resulted in high identification accuracy (97.57% to 99.72%) for histopathology pictures with resolutions ranging from 80×80 pixels to 160×160 pixels.

The experimental results demonstrated that ensemble models may extract key information even from smaller picture patches while retaining good performance. This improvement implies the possibility of adopting digital scanners with lower specifications, as well as reduced data storage and computing needs for histopathology operations. This, in turn, might speed up stomach cancer identification and perhaps increase survival rates. Continued work in these areas is intended to push the boundaries of medical image processing and enhance clinical results.

However, it is critical to recognize the limits of the current research. The usage of a restricted dataset emphasizes the need to have access to larger, higher-quality datasets to enhance and confirm the approaches. Furthermore, computational restrictions may have influenced the scope of the results. Future studies might look at introducing new preprocessing methods and optimizing algorithms to boost performance. Furthermore, the field of medical image retrieval offers several chances for continuous research, including the ability to use multiple deep-learning approaches and models for complete examination.

Supplementary Materials: The following supporting information can be downloaded at the website of this paper posted on Preprints.org. The GasHisSDB dataset is openly available at this Link: <https://paperswithcode.com/dataset/gashissdb>.

Funding: This research received no funding.

Institutional Review Board Statement: Not applicable.

Informed Consent Statement: Informed consent was obtained from all subjects involved in the study.

Data Availability Statement: Not applicable.

Acknowledgments: We would like to express our deepest gratitude to the Roux Institute, the IEAI and the Alfond Foundation for their invaluable support and contributions.

Conflicts of Interest: The authors declare no conflict of interest.

References

1. Rai, H.M. Cancer detection and segmentation using machine learning and deep learning techniques: a review. *Multimed Tools Appl* 83, 27001–27035 (2024). <https://doi.org/10.1007/s11042-023-16520-5>
2. Sara Kuntz, Eva Krieghoff-Henning, Jakob N. Kather, Tanja Jutzi, Julia Höhn, Lennard Kiehl, Achim Hekler, Elizabeth Alwers, Christof von Kalle, Stefan Fröhling, Jochen S. Utikal, Hermann Brenner, Michael Hoffmeister, Titus J. Brinker, "Gastrointestinal cancer classification and prognostication from histology using deep learning: Systematic review", European Journal of Cancer, Volume 155, 2021, Pages 200-215, ISSN 0959-8049, <https://doi.org/10.1016/j.ejca.2021.07.012>.
3. O. M. Mirza, A. Alsobhi, T. Hasarin, M. K. Ishak, F. K. Karim and S. M. Mostafa, "Computer Aided Diagnosis for Gastrointestinal Cancer Classification Using Hybrid Rice Optimization With Deep Learning," in IEEE Access, vol. 11, pp. 76321-76329, 2023, doi: 10.1109/ACCESS.2023.3297441.
4. Suzuki, H., Yoshitaka, T., Yoshio, T., & Tada, T. (2020). Artificial intelligence for cancer detection of the upper gastrointestinal tract. *Diseases of the Esophagus*, 1-6. <https://doi.org/10.1111/den.13897>
5. F. Yasmin et al., "GastroNet: Gastrointestinal Polyp and Abnormal Feature Detection and Classification With Deep Learning Approach," in IEEE Access, vol. 11, pp. 97605-97624, 2023, doi: 10.1109/ACCESS.2023.3312729.
6. Yong MP, Hum YC, Lai KW, Lee YL, Goh CH, Yap WS, Tee YK. Histopathological Gastric Cancer Detection on GasHisSDB Dataset Using Deep Ensemble Learning. *Diagnostics* (Basel). 2023 May 18;13(10):1793. doi: 10.3390/diagnostics13101793. PMID: 37238277; PMCID: PMC10217020.
7. Sivari, E.; Bostanci, E.; Guzel, M.S.; Acici, K.; Asuroglu, T.; Ercelebi Ayyildiz, T. A New Approach for Gastrointestinal Tract Findings Detection and Classification: Deep Learning-Based Hybrid Stacking Ensemble Models. *Diagnostics* 2023, 13, 720.
8. Gunasekaran H, Ramalakshmi K, Swaminathan DK, J A, Mazzara M. GIT-Net: An Ensemble Deep Learning-Based GI Tract Classification of Endoscopic Images. *Bioengineering* (Basel). 2023 Jul 5;10(7):809. doi: 10.3390/bioengineering10070809. PMID: 37508836; PMCID: PMC10376874
9. Qiaosen Su, Fengsheng Wang, Dong Chen, Gang Chen, Chao Li, Leyi Wei, "Deep convolutional neural networks with ensemble learning and transfer learning for automated detection of gastrointestinal diseases", *Computers in Biology and Medicine*, Volume 150, 2022, 106054, ISSN 0010-4825, <https://doi.org/10.1016/j.combiomed.2022.106054>.
10. O. R. A. Almanifi, M. A. M. Razman, I. M. Khairuddin, M. A. Abdullah and A. P. P. A. Majeed, "Automated Gastrointestinal Tract Classification Via Deep Learning and The Ensemble Method," 2021 21st International Conference on Control, Automation and Systems (ICCAS), Jeju, Korea, Republic of, 2021, pp. 602-606, doi: 10.23919/ICCAS52745.2021.9649754. keywords: {Deep learning;Automation;Stacking;Predictive models;Control systems;Gastrointestinal tract;Data models;Gastrointestinal tract;Colorectal cancer;Deep learning;CNN;Transfer learning;Ensemble}
11. Haile, M. B., Salau, A. O., Enyew, B., Belay, A. J., & Jin, Z. (2022). Detection and classification of gastrointestinal disease using convolutional neural network and SVM. *Cogent Engineering*, 9(1). <https://doi.org/10.1080/23311916.2022.2084878>
12. Billah, M.; Waheed, S. Gastrointestinal polyp detection in endoscopic images using an improved feature extraction method. *Biomed. Eng. Lett.* 2018, 8, 69–75. [Google Scholar] [CrossRef] [PubMed]
13. Chao, W.L.; Manickavasagan, H.; Krishna, S.G. Application of Artificial Intelligence in the Detection and Differentiation of Colon Polyps: A Technical Review for Physicians. *Diagnostics* 2019, 9, 99. [Google Scholar] [CrossRef] [PubMed]
14. Li, B.; Meng, M.Q.H. Automatic polyp detection for wireless capsule endoscopy images. *Expert Syst. Appl.* 2012, 39, 10952–10958. [Google Scholar] [CrossRef]
15. Guo, L.; Gong, H.; Wang, Q.; Zhang, Q.; Tong, H.; Li, J.; Lei, X.; Xiao, X.; Li, C.; Jiang, J.; et al. Detection of multiple lesions of gastrointestinal tract for endoscopy using artificial intelligence model: A pilot study. *Surg. Endosc.* 2021, 35, 6532–6538. [Google Scholar] [CrossRef]
16. Charfi, S.; El Ansari, M.; Balasingham, I. Computer-aided diagnosis system for ulcer detection in wireless capsule endoscopy images. *IET Image Process.* 2019, 13, 1023–1030. [Google Scholar] [CrossRef]
17. Wang, X.; Qian, H.; Ciaccio, E.J.; Lewis, S.K.; Bhagat, G.; Green, P.H.; Xu, S.; Huang, L.; Gao, R.; Liu, Y. Celiac disease diagnosis from videocapsule endoscopy images with residual learning and deep feature extraction. *Comput. Methods Programs Biomed.* 2020, 187, 105236. [Google Scholar] [CrossRef]
18. Renna, F.; Martins, M.; Neto, A.; Cunha, A.; Libânia, D.; Dinis-Ribeiro, M.; Coimbra, M. Artificial Intelligence for Upper Gastrointestinal Endoscopy: A Roadmap from Technology Development to Clinical Practice. *Diagnostics* 2022, 12, 1278. [Google Scholar] [CrossRef]
19. Liedlgruber, M.; Uhl, A. Computer-aided decision support systems for endoscopy in the gastrointestinal tract: A review. *IEEE Rev. Biomed. Eng.* 2011, 4, 73–88. [Google Scholar] [CrossRef]
20. Naz, J.; Sharif, M.; Yasmin, M.; Raza, M.; Khan, M.A. Detection and Classification of Gastrointestinal Diseases using Machine Learning. *Curr. Med. Imaging Former. Curr. Med. Imaging Rev.* 2020, 17, 479–490. [Google Scholar] [CrossRef]

21. Ghazouri, I.; Amal, S.; Ho, V.; Safarnejad, L.; Cabot, J.; Brown-Johnson, C.G.; Leeper, N.; Asch, S.; Shah, N.H.; Ross, E.G. Performance and Usability Testing of an Automated Tool for Detection of Peripheral Artery Disease Using Electronic Health Records. *Sci Rep* 2022, 12, 13364.
22. Singh, A.; Wan, M.; Harrison, L.; Breggia, A.; Christman, R.; Winslow, R.L.; Amal, S. Visualizing Decisions and Analytics of Artificial Intelligence Based Cancer Diagnosis and Grading of Specimen Digitized Biopsy: Case Study for Prostate Cancer. In Proceedings of the Companion Proceedings of the 28th International Conference on Intelligent User Interfaces; Association for Computing Machinery: New York, NY, USA, March 27, 2023; pp. 166–170.

Disclaimer/Publisher's Note: The statements, opinions and data contained in all publications are solely those of the individual author(s) and contributor(s) and not of MDPI and/or the editor(s). MDPI and/or the editor(s) disclaim responsibility for any injury to people or property resulting from any ideas, methods, instructions or products referred to in the content.